

# Radio and X-ray variability of LSI+61<sup>0</sup>303

R. Zamanov<sup>1</sup>, J. Martí<sup>2</sup>, and P. Marziani<sup>1</sup>

<sup>1</sup> INAF, Osservatorio Astronomico di Padova, Vicolo dell'Osservatorio 5, I-35122 Padova, Italy

<sup>2</sup> Departamento de Física, Universidad de Jaén, C/ Virgen de la Cabeza, 2, E-23071 Jaén, Spain

**Abstract.** We tested the ejector-propeller (E-P) model of the Be/X-ray binary LSI+61<sup>0</sup>303 by using the parameters predicted by the model in the calculations of the X-ray and radio variability. The results are: (1) in terms of the E-P model, the X-ray maximum is due to the periastron passage; (2) the radio outburst can be really a result of the transition from the propeller to the ejector regimes; (3) the radio outburst will delay with respect to the X-ray maximum every orbital period. The proposed scenario seems to be in good agreement with the observations.

## 1. Flaring behaviour of LS I+61<sup>0</sup>303

LS I+61<sup>0</sup>303 (V615 Cas, GT0236+620) is a well known Be/X-ray binary with periodic radio outbursts every 26.5 d, assumed to be the orbital period. After the discovery of the radio variability (Gregory & Taylor 1978) and the first model (Maraschi & Treves, 1981), this massive system has been studied extensively since nearly two decades ago.

The flaring radio emission of LS I+61<sup>0</sup>303 has been modeled by Paredes et al. (1991) as synchrotron radiation from an expanding plasmon containing relativistic particles and magnetic fields. According to Zamanov (1995), the genesis of such plasmon can be interpreted as a result of a transition in the accretion regime of the neutron star as it probes different parts of the Be envelope in an eccentric orbit. The proposed transition would be from so called propeller (P) to the Ejector (E) regime. In this context, propeller means

accretion onto the magnetosphere and ejector is often a synonymous of “young radio pulsar”.

Our purpose here is to test the agreement between the plasmon parameters predicted by the theory of a P-E transition and those required to reproduce the observed radio and X-ray variability. We anticipate here that the agreement seems to be good at least qualitatively, including the possibility to explain the X-ray luminosity and variability.

## 2. Simultaneous Radio and X-ray observations

The variability of the source in the X-ray domain was detected by ROSAT (Goldoni & Mereghetti, 1995). The LS I+61<sup>0</sup>303 flaring events have been monitored twice by coordinated radio and X-ray observations. The results were presented in Taylor et al.(1996) and Harrison et al.(2000). The behavior observed is reproduced in Fig. 1.

From this figure, it is clear that in both cases the radio peak is delayed with respect to X-ray maximum.

### 3. Plasmon parameters and radio outbursts

Switching on the ejector will create a cavern around the neutron star. This cavern will start to expand under the pressure of the ejector relativistic wind. It can be identified with the expanding plasmon, whose expected radio emission successfully fit the observed radio outbursts of LS I+61°303 (modeled by Paredes et al. 1991). The question here is: are the parameters expected at the propeller-ejector transition appropriate for the plasmon?

In the terms of E-P model we can put constraints on the allowed ranges for the needed input parameters:

(1) The time of plasmon appearance - the plasmon will appear after the periastron passage at low mass accretion rate (for more details see Zamanov 1995, and references therein). So it means that the radio outbursts will peak always with some phase shift after the change of the regime from propeller to ejector.

(2) The initial radius - The initial radius expected at the propeller-ejector transition will be of the order of the light cylinder radius, and in any case less than the accretion radius, which means that acceptable values are of the order of  $0.01 - 3.0 R_{\odot}$ .

(3) The cavern expansion velocity (Zamanov 1995) - expected to be  $200 - 1300 \text{ km s}^{-1}$ . In the radio light curves we will adopt values  $V_{\text{exp}} = 200, 400, 1200 \text{ km s}^{-1}$ .

(4) Injection time interval - it is the time neutron star acts as ejector. From Fig.3) we can expect injection time interval  $0.4 - 0.7 \times P_{\text{orb}}$  or in other words  $10 - 20$  days.

(5) Injection rate - the total injection rate of the Crab into the nebula at a spin period of  $0.033 \text{ s}^{-1}$  is estimated to be about  $10^{40} - 10^{41}$  particles  $\text{s}^{-1}$  on base of the high-energy spectrum (De Jager & Harding, 1992). From one side the spin period of

the neutron star in LS I+61°303 required from the E-P model is longer than that of Crab. We expect  $P_{\text{spin}} = 0.15 - 0.20 \text{ s}$  (see Zamanov 1995 for more details). It means  $\sim 100 - 1000$  times a lower rate of injected relativistic particles ( $L_m \sim P_{\text{spin}}^{-4}$ ). On the other hand, as a result of the magnetosphere accretion there are probably more particles for injection. We will adopt  $5 \times 10^{-38} \text{ e}^{-} \text{ s}^{-1}$ .

(6) Magnetic field - the origin of magnetic field inside the plasmon will resemble the one of the Crab magnetic field but, in LS I+61°303, some additional contribution from the B star is possible. The magnetic field labeled in the “radio” figures (Fig.4) are very high because they refer to the magnetic field at the initial plasmon radius. When the plasmon expands to sizes of 1 AU, as measured with VLBI, the magnetic field is then close to 1 Gauss. This is in agreement with VLBI estimates based on equipartition arguments. (Note: Changes in the radius and the magnetic field do not alter the light curves provided that  $B R^2$  is constant - magnetic flux conservation).

(7) The electron energy power law index is adopted  $p = 1.6$ , in order to be consistent with observed non-thermal (i.e. negative) spectral indices when the plasmon becomes optically thin. According to synchrotron theory, the optically thin spectral index is  $\alpha = (1 - p)/2$ . In our case, we have then  $\alpha = -0.3$  in agreement with typical observations.

(8) Energy range of relativistic electrons:  $m_e c^2 < E < 10^{-2} \text{ erg}$

(9) Distance from the Earth: 2 kpc

Using the above parameters appropriate for the E-P model and the plasmon prescription we generated radio light curves. They are shown in Fig.4.

### 4. Discussion

The general shape of the X-ray and radio variability of the Be/X-ray binary LS I+61°303 calculated in terms of the Ejector-Propeller model is very similar to the observed one. The radio outbursts peak

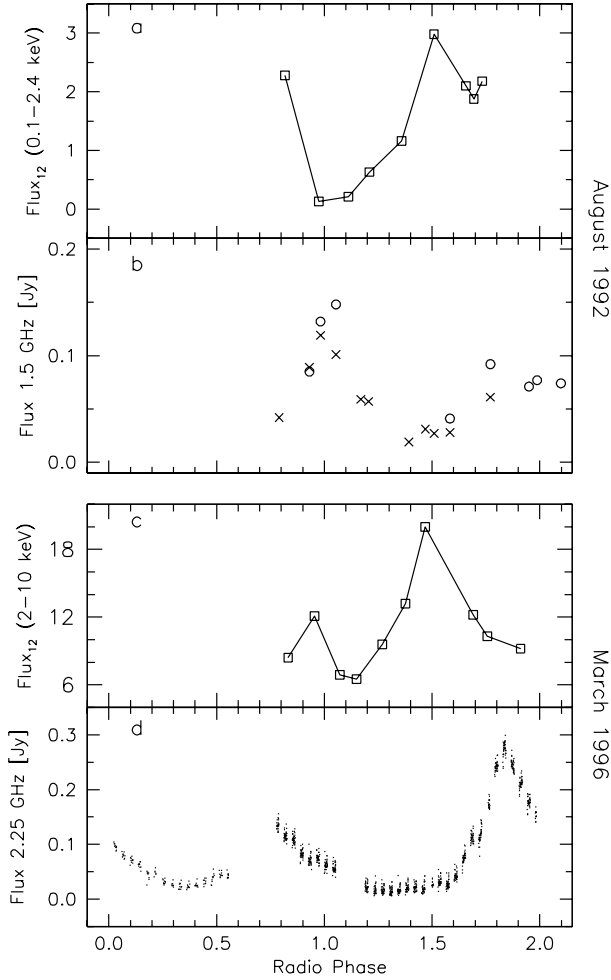


**Fig. 1.** The simultaneous X-ray and radio observations: **(a)** and **(b)** – Taylor et al. (1996) **(c)** and **(d)** – Harrison et al. (2000) The X-ray flux is everywhere in units  $10^{-12}$  erg  $\text{cm}^{-2}$   $\text{s}^{-1}$ . We used the late radio phase ephemeris  $P = 26.4917 d$  and phase zero at JD2443366.775 (Gregory, Peracaula & Taylor, 1999), although a bit shorter orbital period is possible (Leahy 2001). In **(b)** the triangles refer to 1.5 GHz and the crosses – to 4.9 GHz flux density.

A clear phase shift between X-ray and radio is visible in both cases. Our model is the only one explaining this shift in a natural way.

can be achieved 2-8 days after the appearance of the plasmon (see Fig.4). The appearance of the plasmon can be expected when the neutron star emerges from the denser part of the disk, i.e. 2–5 days after

the periastron (orbital period is 26.5 days). In the calculated X-ray curves the X-ray maximum corresponds to the periastron. The ejector will switch on at  $0.1 - 0.4 P_{orb}$  later. It means that the radio peak will de-

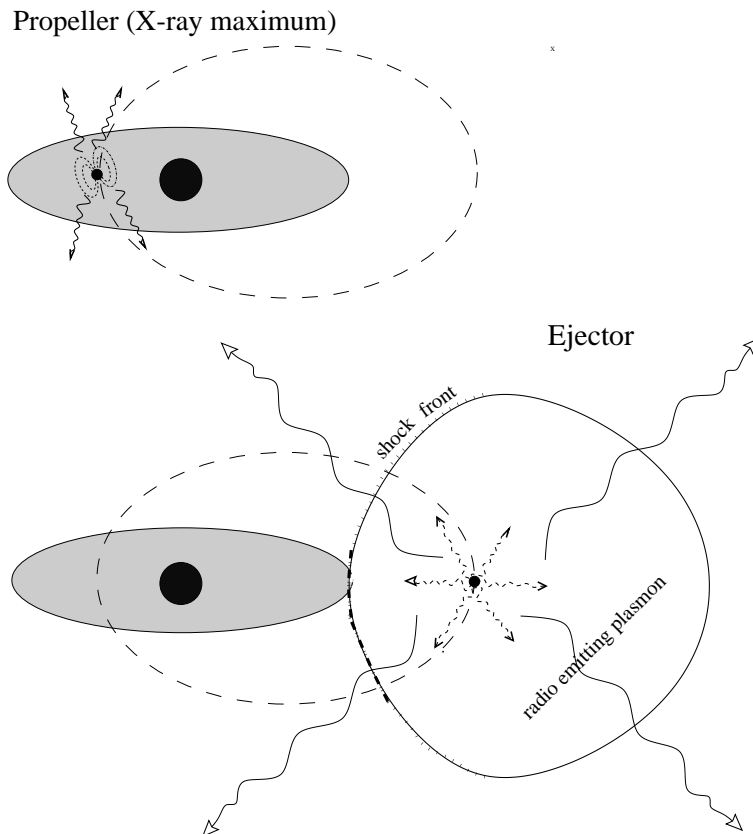


**Fig. 2.** A sketch of the Ejector-propeller model. The dashed lines indicates the orbit of the neutron star. Upper panel - accretion onto the magnetosphere at periastron, lower panel - ejector and the cavern around the neutron star.

lay with 3-13 days after the X-ray maximum. This is the behavior observed in both cases of the simultaneous radio and X-ray observations (Fig.1).

**High resolution radio maps:** Recent high resolution radio maps have evidenced a one sided radio jet at milliarcsecond scales (Massi et al. 2001). These authors interpret it as a microquasar bipolar ejection with significant Doppler boosting effect. The ejector-propeller model, explored in this paper, provides however an alternative interpretation. Considering that the plasmon will be formed in one side of the Be star (the apastron vicinity), a one sided radio jet is naturally expected.

**Asymmetry of the cavern:** To model the radio light curves we assumed that the plasmon expansion is spherically symmetric. But in the real case this region will be not symmetric. Different forms of the cavern are possible - closed or open, for more details see Lipunov & Prokhorov (1984). In addition, the fact that the neutron star ejects relativistic particles at the apastron of an eccentric orbit will lead to a radio source which is elongated in the direction of apastron. In any case, the radio source formed around the ejecting neutron star will be elongated in the direction opposite to the direction to the B star.

**Strong and weak radio outbursts:** It was discovered that radio outburst peak

flux density varies over a time scale of 1600 days. On the same time scale the  $H\alpha$  emission of the outflowing disk (Zamanov & Marti, 2000) varies as well, and may be even the X-ray maximum (Apparao 2001). Our preliminary tests evidenced that a slower expansion velocity and stronger magnetic field give higher radio peak flux densities and that the outburst peaks later. Also a faster expansion velocity and lower magnetic field will result into lower peak flux densities and earlier outburst peaks. These effects and their connection with the conditions in the Be disk need of carefully modeled.

**Multiple Outbursts:** A mechanism of multiple formation of caverns around an ejecting neutron star has been proposed by Lipunov & Prokhorov (1984). We can speculate that, in case of multiple peaks in the LS I+61°303 radio outbursts, we may be observing such a multiple cavern formation. Another possibility is density structures in the wind of the Be star, i.e. rings with higher density that can change the regime more than once during an orbital period.

**Other possibilities:** An alternative to the proposed model is the transition closed-open cavern around the ejecting neutron star (Zamanov 1995b, Harrison et al. 2000). It cannot be excluded that a magnetized black hole is acting in LS I+61°303 (Punsly, 1999). If such a compact object does exist in LS I+61°303, the microquasar scenario proposed by Massi et al. (2001) should be also considered seriously. Further observations are required in order to finally solve the true nature of this X-ray binary. High resolution maps could help us to understand the birth and the initial expansion of the plasmon.

## 5. Conclusions

We tested the ejector-propeller model for the radio-emitting Be/X-ray binary LS I+61°303. The calculations show that the X-ray variability and radio outbursts can be the result of the transition from the

propeller to the ejector accretion regimes every orbital period. The main results are:

- The parameters expected from the ejector-propeller model are appropriate for the radio plasmon and the calculated radio light curves are similar to the observed radio outbursts in LS I+61°303.

- In terms of Ejector-Propeller model the X-ray maximum is a result of the propeller action during the periastron passage of the neutron star.

- The periastron is expected to correspond with radio phase  $\sim 0.5$  using the latest radio ephemeris i.e., the time of the X-ray maximum.

- The observed phase shift between the radio and the X-ray maximum is in agreement with the ejector-propeller model of LS I+61°303. We expect that the X-ray and the radio maxima will always peak at different orbital phase.

- The total X-ray luminosity expected in terms of Ejector -Propeller model  $1 - 200 \times 10^{33} \text{ ergs}^{-1}$  is in good agreement with the observed by ASCA (Paredes et al. 1997) variability  $1 - 6 \times 10^{34} \text{ ergs}^{-1}$  in the 2-10 keV band.

## References

- Apparao K.M.V., 2001, A&A 371, 672  
 De Jager O.C., Harding A.K., 1992, ApJ 396, 161  
 Goldoni P., Mereghetti S., 1995, A&A 299, 751  
 Gregory P.C., Peracaula M., Taylor A.R., 1999, ApJ 520, 376  
 Gregory P.C. & Taylor A.R., 1978, Nature 272, 704  
 Harrison F.A., Ray P.S., Leahy D.A., et al., 2000, ApJ 528, 454  
 Leahy D.A., 2001, A&A 380, 516  
 Lipunov V.M., Prokhorov M.E., 1984, Ap&SS 98, 221  
 Maraschi L. & Treves A., 1981, MNRAS 194, 1p  
 Massi M., Ribo M., Paredes J. et al., 2001, A&A, 376, 217  
 Paredes J.M., Martí J., Estalella R., Sarrate J., 1991, A&A 248, 12

- Paredes J.M., Martí J., Peracaula M., Ribó M., 1997, A&A 320, L25  
Punsly B., 1999, ApJ 519, 336  
Taylor A.R., Young G., Peracaula M., et al. 1996, A&A 305, 817  
Zamanov R., 1995a, MNRAS 272, 308  
Zamanov R., 1995b, Comp. Rend. Acad. bulg.Sci. 48, N: 5, 5  
Zamanov R., Marti J., 2000, A&A 358, L55

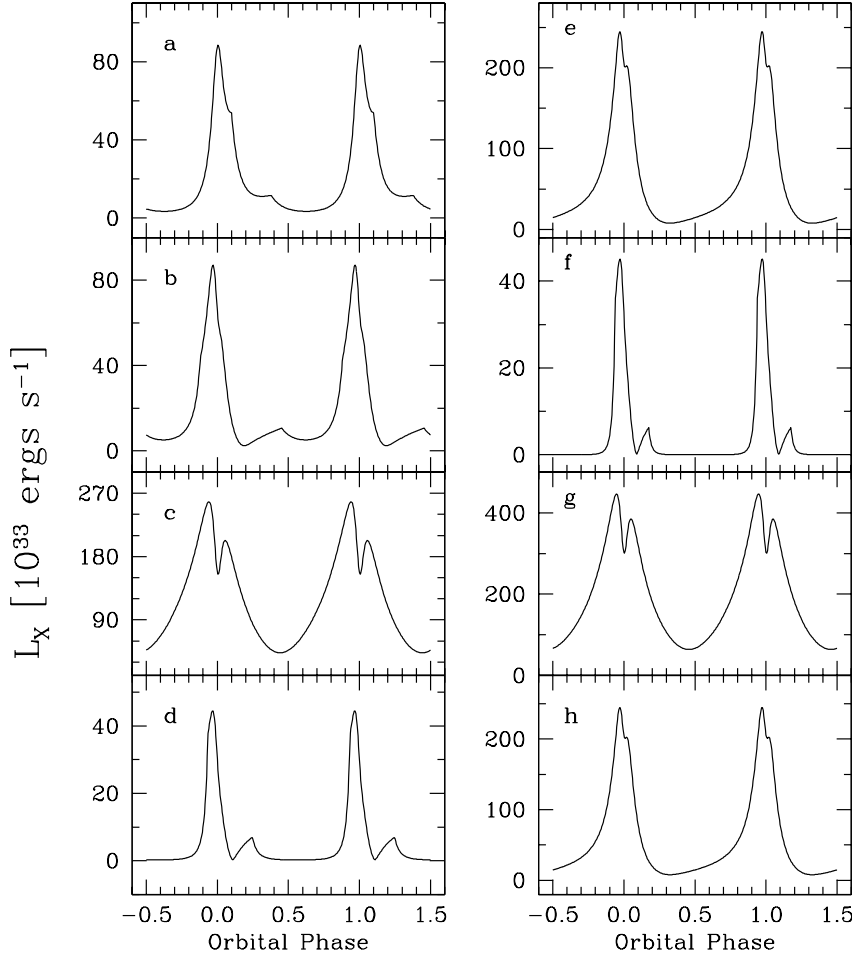


**Fig. 3.** The calculated X-ray luminosity of the the neutron star in LS I+61°303 using different wind parameters. The  $L_X$  is calculated as magnetospheric accretion luminosity and supposing that  $L_X(ejector) = L_X(propeller)$ . The radio outbursts are expected to peak after the X-ray maximum, when the mass accretion rate is lower, and the NS can change its regime from propeller to ejector.

(a)  $V_0=5 \text{ km s}^{-1}$ ,  $n = 3.25$ , non-rotating disk,  $\overline{\dot{M}}_a = 0.09 \dot{M}_{loss}$

(b)  $V_0=5 \text{ km s}^{-1}$ ,  $n = 3.25$ , keplerian disk,  $\overline{\dot{M}}_a = 0.08 \dot{M}_{loss}$

(c)  $V_0=10 \text{ km s}^{-1}$ ,  $n = 2.1$ , keplerian,  $\overline{\dot{M}}_a = 0.36 \dot{M}_{loss}$

(d)  $V_0=10 \text{ km s}^{-1}$ ,  $n = 3.25$ , keplerian,  $\overline{\dot{M}}_a = 0.03 \dot{M}_{loss}$

(e)  $V_0=2 \text{ km s}^{-1}$ ,  $n = 3.25$ , keplerian,  $\overline{\dot{M}}_a = 0.20 \dot{M}_{loss}$

(f)  $V_0=5 \text{ km s}^{-1}$ ,  $n = 3.75$ , keplerian,  $\overline{\dot{M}}_a = 0.02 \dot{M}_{loss}$

(g)  $V_0=5 \text{ km s}^{-1}$ ,  $n = 2.25$ , keplerian,  $\overline{\dot{M}}_a = 0.53 \dot{M}_{loss}$

(h)  $V_0=2 \text{ km s}^{-1}$ ,  $n = 3.25$ , keplerian,  $\overline{\dot{M}}_a = 0.20 \dot{M}_{loss}$

Everywhere we adopted mass loss rate in the outflowing disk  $\dot{M}_{loss} = 10^{-9} M_\odot \text{ yr}^{-1}$  and eccentricity  $e = 0.6$ .

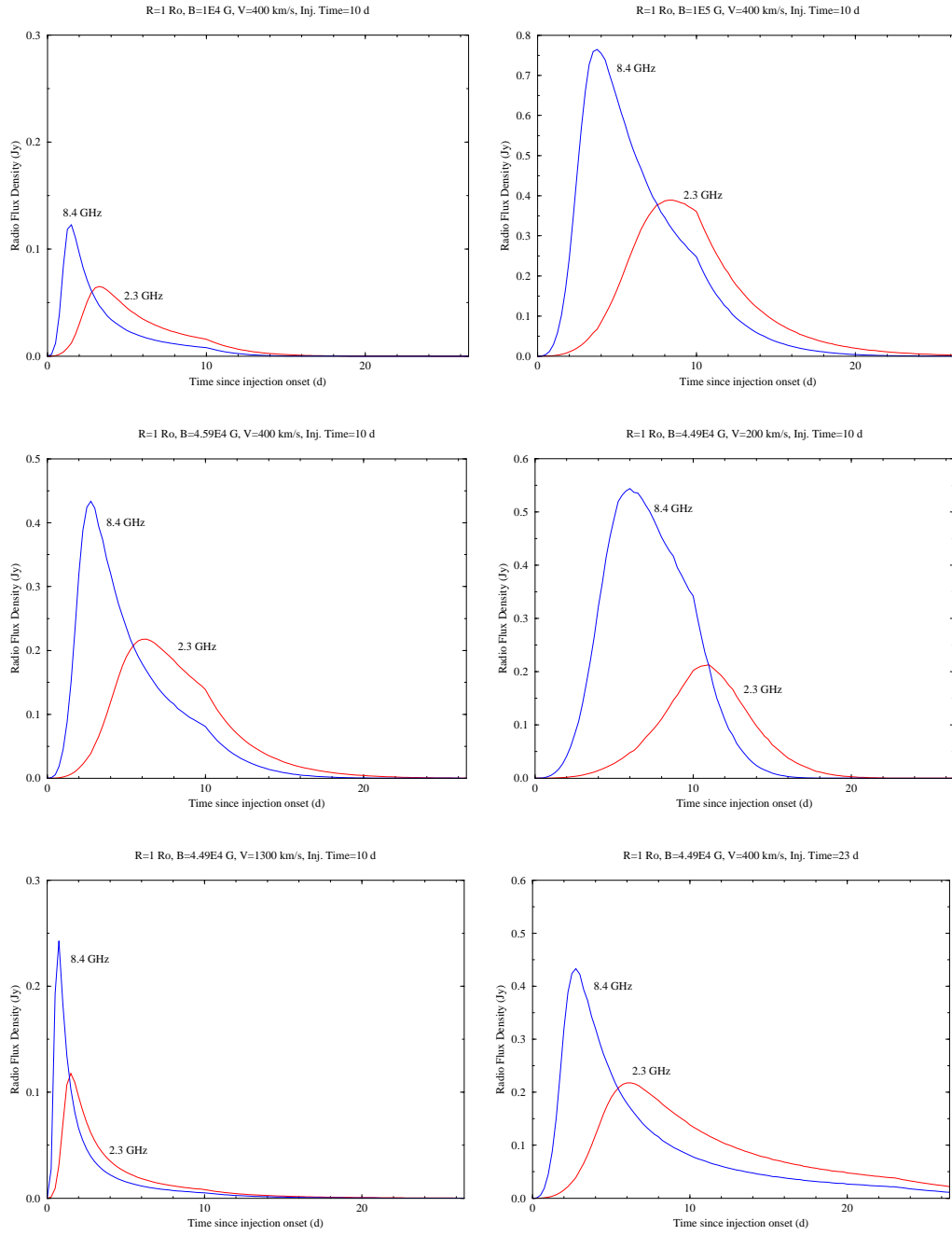


**Fig. 4.** Simulated Radio Light curves with parameters for the expanding plasmon set to be appropriate for the ejector-propeller model.